

---

# **International Journal of Low Carbon Technologies**



---

**1/2**

---

**April 2006**

---

Editor-in-chief

Professor S. B. Riffat

---

# Activated carbon fiber composites for ammonia, methane and hydrogen adsorption

L. L. Vasiliev<sup>1</sup> (corresponding author), L. E. Kanonchik<sup>1</sup>, A. G. Kulakov<sup>1</sup>, D. A. Mishkinis<sup>1</sup>, A. M. Safonova<sup>2</sup> and N. K. Luneva<sup>2</sup>

<sup>1</sup> Luikov Heat and Mass Transfer Institute, Minsk, Republic Belarus

E-mail: IVASIL@hmti.ac.by

<sup>2</sup> Institute of General and Inorganic Chemistry Minsk, Republic Belarus

**Abstract** Complex compound material (activated carbon fiber, saturated with salts, or metal hydrides) was developed as an efficient gas (ammonia, methane, hydrogen) adsorbent for new gas storage and transportation system application. To enhance the performance and thermodynamic efficiency of the gas storage vessels a heat pipe thermal control system was suggested.

**Keywords** adsorption; activated carbon fiber; metal chlorides; metal hydrides; gas storage system

## Nomenclature

$a$	adsorption capacity	kg/kg
$a_v$	volume capacity of hydrogen storage using physisorption	m <sup>3</sup> /kg
$C$	density of free gas	kg/m <sup>3</sup>
$C$	solid sorbent specific heat capacity	J/(kg·K)
$C_g$	specific heat capacity of free gas	J/(kg·K)
$C_a$	specific heat capacity of adsorbed gas	J/(kg·K)
$E$	activation energy	J/kg
$G$	gas output from the cylinder	kg/sec
$g_1$	gas output from the elementary cell, used for computer modeling	kg/sec
$K_{s0}$	pre-exponent constant in the equation of kinetic of sorption	s <sup>-1</sup>
$M$	mass of the gas in the cylinder	kg
$M_i$	mass of the gas in the calculated cell	kg
$N$	number of calculated cells in the cylinder	
$P$	pressure	Pa, MPa
$q_{st}$	latent (isosteric) heat of sorption	J/kg
$Q$	heat flow	W
$r, z$	cylindrical coordinates	m
$R$	external radius of the cylinder shell	m
$R_0$	internal radius of the heat pipe	m
$r_0, r$	internal and external radii of the annular layer of the sorbent	m
$R_\mu$	gas constant	J/(kg·K)
$R_p$	mean radius of the particles	m
$2S$	finning step	m
$T$	temperature	K, °C
$W_0$	maximum microporous specific volume	m <sup>3</sup> /kg
$v$	component of the velocity vector	m/sec
$v_a$	specific volume of adsorbed medium	m <sup>3</sup> /kg

*Greek Letters*

$\alpha$	coefficient of heat transfer	$W/(m^2 \cdot K)$
$\varepsilon$	porosity determined as a part of the volume occupied by the free gas (not bound by adsorption)	
$2\delta$	fin thickness	m
$\lambda$	effective thermal conductivity of the sorbent layer	$W/(m \cdot K)$
$\rho_s$	density of the solid sorbent	$kg/m^3$
$\rho$	total density of the free and adsorbed gases in the cylinder	$kg/m^3$
$\rho_v$	volume density of storage	$m^3(STP)/m^3$
$\tau$	time	sec

*Subscripts*

<i>a</i>	adsorbate
<i>cr</i>	critical state
<i>e</i>	finite value
<i>eq</i>	equilibrium conditions
<i>env</i>	environment
<i>f</i>	fin
<i>hp</i>	heat pipe
<i>0</i>	initial value
<i>s</i>	sorbent

*Abbreviation*

GSV	gas storage vessel (GSV)
HP	heat pipe
HPP	heat pipe panel
STP	standard of temperature (273 K) and pressure (0.1 MPa)

**1. Introduction**

Activated carbon is well known as one of the best adsorbents for gases [1–3]. In contrast to the metal hydrides chemisorption [4], the phenomenon of physical adsorption is essentially accumulation of the undissociated hydrogen molecules on a surface of microporous carbon fibers or particles. This property is due to the fact that the carbon could be prepared in a very fine powdered or fiber form with highly developed porous structure and due to specific nature of the interactions between carbon atoms and gas molecules. The total amount of the adsorbed hydrogen strongly depends on the pore geometry and pore size distribution as well as the storage pressure and temperature levels. Recently many improvements have been accomplished to obtain microporous carbonaceous materials with very high adsorbing properties for different gases [5]. Adsorption of such gases as ammonia, methane and hydrogen usually takes place in micropores. Macropores have no practical influence on the adsorption capacity. They are only important for the gas compression and for adsorption/desorption reaction rates [6]. Thanks to its high specific surface area and abundant pore volume, the activated carbon could be considered as

advanced and fast reaction adsorbent. For the conventional activated carbon, the hydrogen uptake as a rule is proportional to the surface area and pore volume, while, unfortunately, a high hydrogen adsorption capacity ( $0.04 \sim 0.06 \text{ kg/kg}$ ) can be only obtained at very low cryogenic temperatures according to theoretical calculations. To gain the goal of the problem – efficient ammonia, methane, and hydrogen storage and transportation it is necessary to develop a high performance microporous adsorbent material and an advanced system of the vessel thermal control.

The inexpensive activated carbon fabricated by special thermal treatment of impregnated raw (wood, sawdust, cellulose, straw, paper for recycling, peat etc.) is of special interest for modern sorption technologies. The use of particular organic and non-organic compounds as raw impregnates gives possibility of activated carbon production with controlled porous structure and high yield (up to  $0.5 \text{ kg/kg}$ ). Developed advanced technology allows producing the homogeneous carbon adsorbents with benzene pore volume  $0.3 \cdot 10^{-3} - 0.6 \cdot 10^{-3} \text{ m}^3/\text{kg}$  (70–80% is the volume of micropores), nitrogen specific surface area up to  $1500 \text{ m}^2/\text{g}$ , iodine adsorption capacity  $0.4 - 0.7 \text{ kg/kg}$  and methane adsorption capacity up to  $0.16 \text{ kg/kg}$  (3.5 MPa, 293 K). Impregnated cellulose – based raw is the attractive host material for the manufacture of special activated carbons for ammonia, methane and hydrogen storage systems with high microporosity, specific surface area and narrow micropore size distribution. The activated carbon fiber 'Busofit' and activated wood-based carbon pellets [7] fabricated in Belarus are prospective materials for gas storage systems (Figures 1–2). The Figures 1(a) and 2(a) were obtained by electron microscope scanning. To get Figures 1–2 an optical scanning microscope technique was also used.

'Busofit' is capable of effectively adsorbing a number of different gases ( $\text{H}_2$ ,  $\text{N}_2$ ,  $\text{O}_2$ ,  $\text{CH}_4$ , and  $\text{NH}_3$ ). The texture of the active carbon fiber filament is shown on Figures 2(a), (b) and (c). The material can be performed as a loose fibers bed or felt or as monolithic blocks with a binder to ensure a good thermal conductivity.

To be commercially profitable the natural gas adsorption storage is required to have at least 150 volumes of methane per volume of the vessel. Several samples of activated carbon fiber 'Busofit' produced and treated by the new technologies were

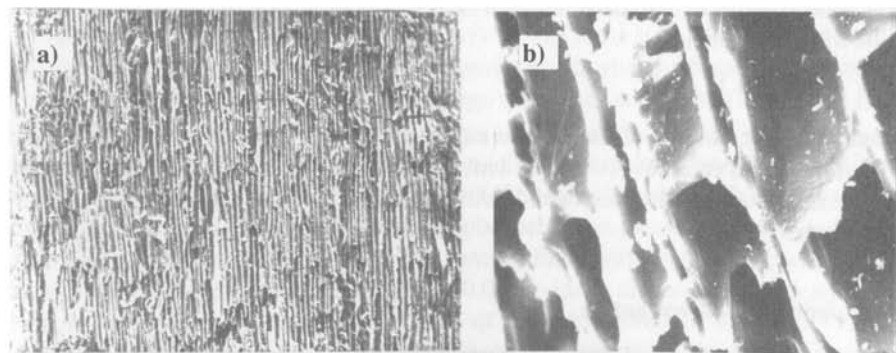


Figure 1. Active carbon material made from waste wood (IGIC NASB): a) Image multiplied by 30 times; b) by 1000 times.

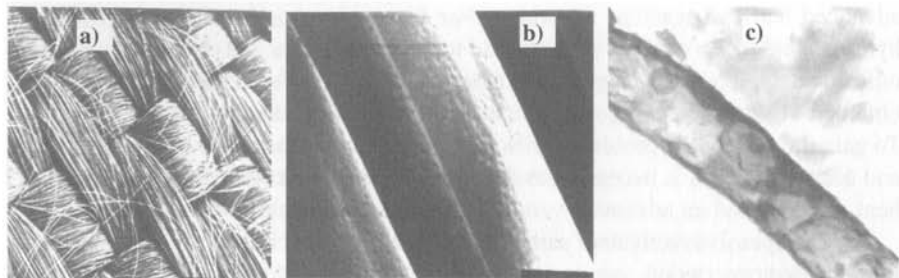


Figure 2. Active carbon fiber 'Busofit': a) Image multiplied by 50 times; b) by 1000 times; c) by 50,000 times.

investigated. The specific surface area of the commercially available 'Busofit' was measured by 'Micromeritics AccuSorb 2100' and BET Sorbtometer NOVA and varied from  $1140 \text{ m}^2/\text{g}$  up to  $1570 \text{ m}^2/\text{g}$ . Ammonia, methane and hydrogen storage vessels filled with 'Busofit' have certain advantages (methane storage capacity is near 170 volumes per volume of the vessel at pressure 3.5 MPa). It is a typical microporous adsorbent with average pore diameter near  $(1-2) \cdot 10^{-9} \text{ m}$ , and at the same it has high gas permeability.

The micropores formation and distribution is performed mostly on the carbon surface of filament. Nowadays research program was undertaken to examine the parameters of an active carbon fiber for optimization of the gas (ammonia, methane and hydrogen) mass uptake, and the material density.

'Busofit' has the following advantages:

- high rate of adsorption and desorption;
- uniform pore distribution  $(0.6-1.6) \cdot 10^{-9} \text{ m}$  on the surface of filament;
- small number of macropores  $(100-200) \cdot 10^{-9} \text{ m}$  with its specific surface area  $0.5-2 \text{ m}^2/\text{g}$ ;
- limited number of mesopores with its specific surface area  $50 \text{ m}^2/\text{g}$ .

The total volume  $V$ , associated with an active carbon adsorbent can be divided into following components:

$$V = V_c + V_v + V_{\text{void}} + V_{\mu}, \quad (1)$$

where  $V_c$  – the volume of the carbon atoms, of which the adsorbent is composed;  $V_{\mu}$  – micropores volume;  $V_v$  – meso- and macropores volume;  $V_{\text{void}}$  – the space inside the vessel free from adsorbent bed. Making the solid block of adsorbent could eliminate latter  $V_{\text{void}}$ .

## 2. Experimental investigation

Activated carbon fibers 'Busofit' and granular activated carbons (additionally activated by authors and commercially available) have been tested using standard nitrogen ( $\text{N}_2$ ) physisorption technology at 77 K and up to a pressure of 0.1 MPa. The  $\text{N}_2$

Table 1. *Textural characteristics and hydrogen-sorption capacities at 77 K and 0.1 MPa for the researched carbon materials*

No.	Sorbent	$a_v \cdot 10^3$ , m <sup>3</sup> (STP)/kg	$a_H$ , kg/kg	$S_H$ , m <sup>2</sup> /g	$S_{BET}$ , m <sup>2</sup> /g	$S_{DR}$ , m <sup>2</sup> /g	$V_{DR} \cdot 10^3$ , m <sup>3</sup> /kg	$R_{DR} \cdot 10^8$ , m
1	Busofit 191-5	199.9	0.0176	462	1691	2496	0.887	49.9
2	Busofit-M2	203.9	0.0179	465	1702	2507	0.89	41.5
3	Busofit-M4	225.1	0.0198	536	1715	2547	0.9	42
4	<b>Busofit-M8</b>	<b>252.9</b>	<b>0.0223</b>	<b>571</b>	<b>1939</b>	<b>2985</b>	<b>1.04</b>	<b>51</b>
5	WAC 97-03	115	0.0101	271	715	1050	0.37	33.4
6	WAC 19-99	172.1	0.0151	393	1005	1486	0.53	41.7
7	<b>WAC 3-00</b>	<b>221.1</b>	<b>0.0195</b>	<b>575</b>	<b>1383</b>	<b>2142</b>	<b>0.74</b>	<b>50</b>
8	207C	209.2	0.0184	502	1300	1944	0.69	41
9	Norit sorbonorit-3	193.8	0.0171	458	1361	2044	0.73	50
10	Sutcliffe	236.6	0.0208	527	1925	2864	1.02	53.6

Notes: WAC – wood-based active carbon;  $a_v$  – volume capacity of hydrogen storage using physisorption, m<sup>3</sup>/kg;  $a$  – capacity of hydrogen storage using physisorption, kg/kg;  $S_H$  – BET surface area determined on hydrogen, m<sup>2</sup>/g;  $S_{BET}$  – BET surface area determined on nitrogen, m<sup>2</sup>/g;  $S_{DR}$  – surface area, determined on Dubinin-Radushkevich method, m<sup>2</sup>/g;  $V_{DR}$  – micropore volume, determined on Dubinin-Radushkevich method, m<sup>3</sup>/kg;  $R_{DR}$  – size of pore, determined on Dubinin-Radushkevich method, m.

and H<sub>2</sub> sorption isotherms were measured with the High Speed Gas Sorption Analyser NOVA 1200 at 77 K in the pressure range 0–0.1 MPa. From the nitrogen physisorption data, the BET-surface area, total pore volume and microporous volume were determined. Table 1 summarizes the sorption parameters of carbon materials. In our experiments four samples of carbon ‘Busofit-AYTM’ (1–4) and three samples of wood-based carbon (5–7) obtained by new technology were investigated. The activated carbon 207C (8) is fabricated from coconut shell. Samples 9 and 10 are granular activated carbons, specially developed for effective storage of methane. All samples are typical micro- and mesoporous carbon materials. According to data from the Table 1, ‘Busofit-M8’ has the highest specific surface area and micropore volume. ‘Busofit-M8’ has also the best storage capacity for hydrogen (0.253) to compare with other tested samples WAC3-00 (0.221) and 207C (0.237). The results of experiments demonstrate that a large capacity of adsorbed hydrogen by physisorption is typical for sorbents, containing a large volume of micropores and a high BET surface area.

The experimental set-up for investigation of carbon materials sorption capacity at the ambient temperature is shown in Figure 3. The experimental reactor allows determining methane and hydrogen adsorption phenomena at pressure level up to 6 MPa. After each test the reactor was placed to furnace filled with inert gas for sorbent bed regeneration. The cylindrical reactor has 0.025 m inner diameter, 0.4 m length and is used to simulate full-scale conditions of the experiment in the ratio 1:50 to compare with the standard vessel. Thermocouples were attached to the sample to control the process of adsorption. Pressure sensor was used for pressure control/set in the experimental reactor. After the selection of the material with good

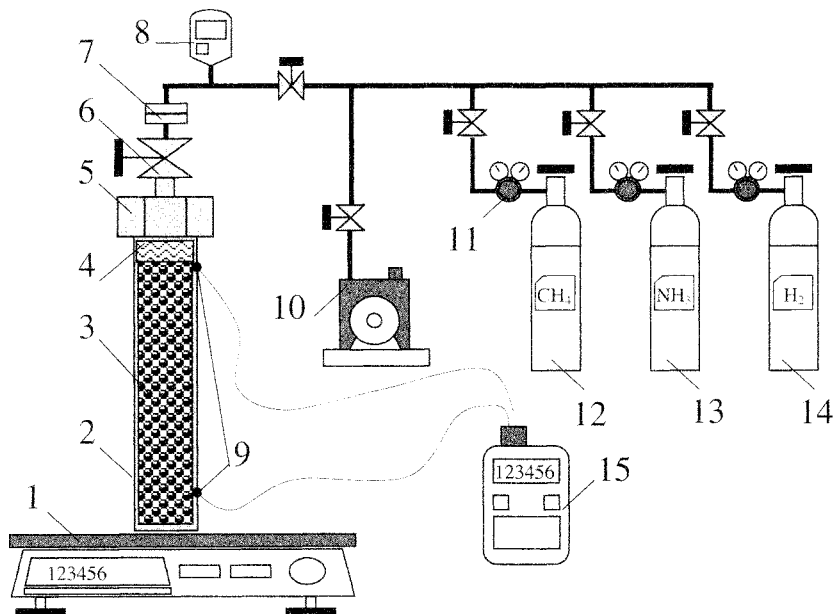


Figure 3. *Experimental apparatus: 1) high precision electronic balances, 2) reactor, 3) sorbent bed, 4) filter (to avoid sorbent particles migration into the system), 5) reactor cap screw, 6) valve, 7) quick-release coupling, 8) pressure sensor, 9) thermocouples, 10) vacuum pump, 11) reducer, 12), 13), 14) cylinders with methane, ammonia and hydrogen, 15) temperature indicator.*

ammonia/methane/hydrogen adsorption properties the detailed sample investigation (with set of isotherms plotting) was accomplished using another experimental setup described in [8].

The rate of the adsorption/desorption of the different gases (ammonia, methane, hydrogen) on the surface of 'Busofit' can be estimated by the isotherms analysis. In order to study the sorption capacity of the material it is necessary to know the quantity of gas adsorbed at each point of the gas storage operational cycle. There is a general need to have a good fit of experimental isotherm and approximating formula and to extrapolate some isotherms beyond the experimental field. For the carbon fiber 'Busofit' the approach of Dubinin is well adapted. It allows relatively easy to link the physical properties of 'Busofit' with the adsorption capacity of the carbon fiber.

As an example, Figure 4 shows the adsorption and desorption experimental isotherms of hydrogen on carbon fiber 'Busofit-M8' and wood-based activated carbon 'WAC 3-00' at the liquid nitrogen temperature. Absence of the noticeable hysteresis confirms reversible physisorption character for investigated materials.

Gas adsorption on microporous carbons can be described with the Dubinin-Radushkevich equation [9]:

$$a_{eq} = \frac{W_0}{v_a} \exp \left\{ - \left[ \frac{R_\mu T \ln(P_{sat}/P)}{E} \right]^2 \right\}. \quad (2)$$

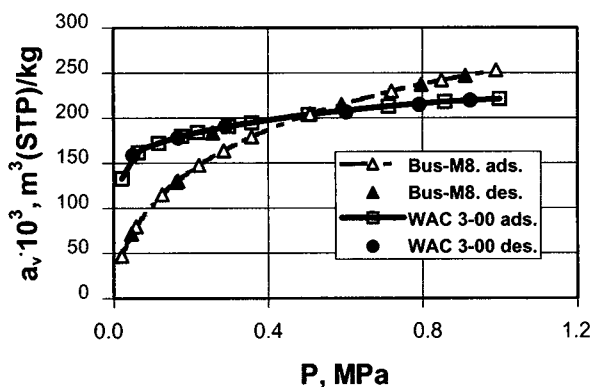


Figure 4. Isotherms of hydrogen adsorption and desorption on carbon materials at temperature 77 K, measured by the High Speed Gas Sorption Analyser NOVA 1200.

Table 2. The empirical coefficients of Dubinin-Radushkevich equation for hydrogen sorption on the carbon materials

Material	$W_0 \cdot 10^3, \text{ m}^3/\text{kg}$	$E, \text{ kJ/kg}$
Busofit-M2	369	1783
Busofit-M4	376	1922
Busofit-M8	482	1710
Sutcliffe	453	1699
WAC 3-00	270	3782
207C	343	1969

The theory of microporous volume filling, suggested by Dubinin, is widely used for quantitative characteristic of porous structure adsorptive properties. Equilibrium state equation (2) includes the saturation pressure  $P_{sat}$ . Since the hydrogen and methane sorption isotherms were measured within the temperature and pressure intervals including the region of supercritical state of the adsorptive, the definition of saturation pressure loses its physical meaning. For this case it was suggested in the work [10] to use following formula for  $P_{sat}$  in equation (2):

$$P_{sat} = P_{cr} (T/T_{cr})^2 \quad (3)$$

The empirical coefficients for the Dubinin-Radushkevich equation (2) obtained from our experimental database are presented in Table 2. With the purpose of selection of hydrogen most suitable adsorbent, the isotherms of studied materials (Figure 5) were compared for pressure level 3.5–6 MPa. This level is of practical



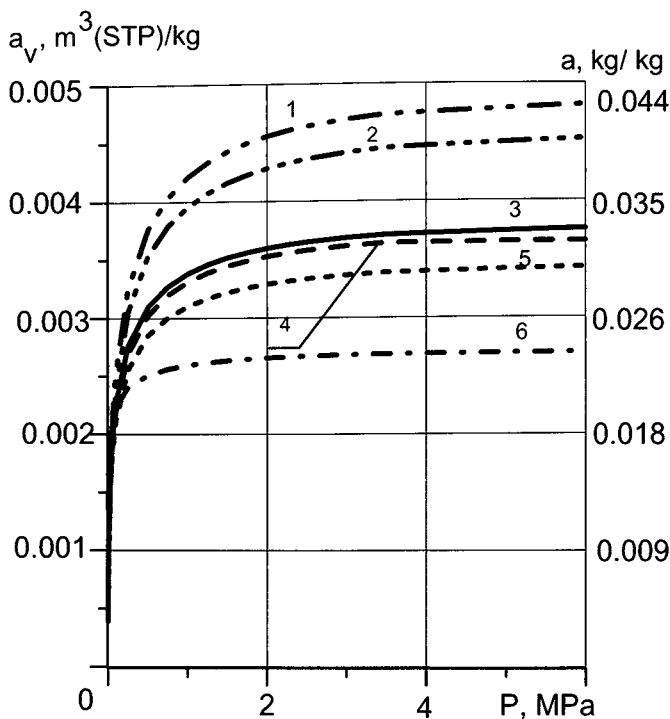


Figure 5. Hydrogen sorption isotherms for the temperature 77K and different carbon materials: 1 – ‘Busofit-M8’, 2 – ‘Sutcliff’, 3 – ‘Busofit-M4’, 4 – ‘Busofit-M2’, 5 – 207C, 6 – ‘WAC 3-00’.

interest for development of onboard storage system. It is obvious, that the best sorbent in the region of liquid nitrogen temperature is the activated fiber ‘Busofit-M8’, having effective porosity (0.78), bulk density of  $500 \text{ kg/m}^3$  and an very high surface area ( $2985 \text{ m}^2/\text{g}$ ). At the pressure 6 MPa ‘Busofit-M8’ reaches  $\text{H}_2$  storage capacity up to  $0.482 \text{ m}^3(\text{STP})/\text{kg}$ . It follows from the analysis of physisorption isotherms, that the wood-based carbon (‘WAC 3-00’) with the greater specific surface area ( $S_{\text{BET}} = 1382 \text{ m}^2/\text{g}$ ) immerses the smaller amount of hydrogen and its isotherm lays below an isotherm of carbon 207C with a specific surface area equal to  $1300 \text{ m}^2/\text{g}$ . The same situation was observed with methane adsorption. Such ‘abnormal’ behaviour testifies more advanced secondary structure meso- and macropores structure presence.

Experimentally obtained methane isotherms evolution during the cycle of adsorption/desorption of ‘Busofit AYTМ’ [11, 12] is shown in Figure 6. Based on these data we can conclude, that ‘Busofit-AYTМ’ is competitive to best activated carbons with methane adsorption capacity 113–135  $\text{kg/kg}$  at 273 K.

Figures 7(a) and (b) show ammonia sorption isotherms for the active carbon fiber ‘Busofit’ and complex compound ‘Busofit +  $\text{CaCl}_2$ ’. All isotherms are experimen-

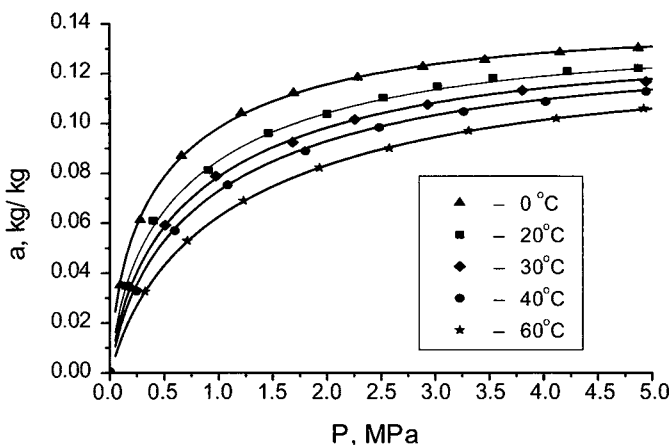


Figure 6. Methane sorption isotherms for active carbon fiber 'Busofit': experimental data – points; calculated data (Dubinin-Radushkevich equation) – lines.

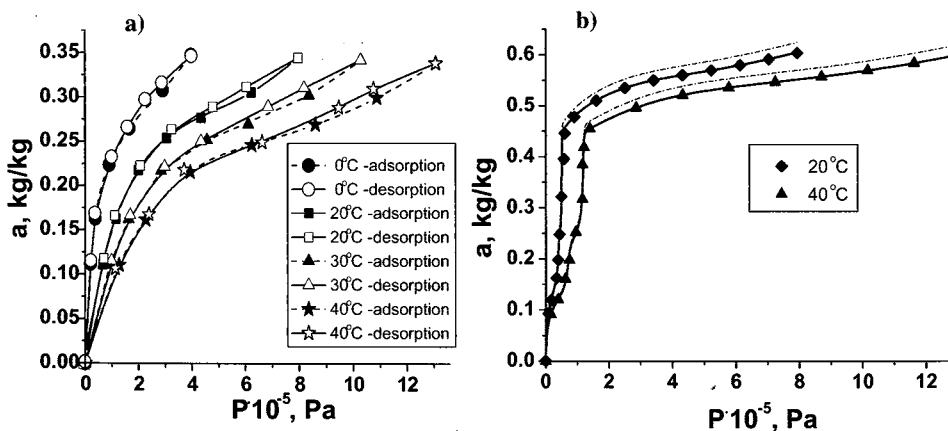


Figure 7. Ammonia sorption isotherms for 'Busofit' (a) and 'Busofit+  $\text{CaCl}_2$ ' (b): experimental data – points; calculated data (Dubinin-Radushkevich equation) – lines.

tally obtained, and experimental setup was described in [8]. Two dashed lines on Figure 7(b) are simulation. The simulation is based on the suggestion that all the impregnated chloride took part in the reaction and 'Busofit' doesn't change its adsorption properties after  $\text{CaCl}_2$  impregnation. As it is seen from plots (Figures 6, 7) experimental data fit the calculated adsorption values (Dubinin-Radushkevich equation) with an error sufficient for practical purposes. The most important feature of this complex compound is related to the fact that we apply two different sorbent materials (one very fast – active carbon, the second not so fast, but with a big sorption capacity – salt) in the same sorbent canister. It results

Table 3. *Full sorption capacity of a sorbent bed*

Full sorption capacity of the sorbent bed, kg/kg	Busofit	Activated Carbon Fiber Composite
Methane, T = 253 K, P = 6 MPa	0.21	
Ammonia	0.35	0.62–1.03 (Busofit + CaCl <sub>2</sub> )
Methanol	0.55	
Hydrogen	0.015	0.032 (Busofit + LaNi <sub>4.5</sub> Al <sub>0.29</sub> Mn <sub>0.21</sub> )

in very interesting interactions between the sorbent materials as a function of time, temperature and pressure. Adsorbents could assist each other to realize an efficient thermal cycle with large gas storage sorption capacity.

### 3. Activated carbon fiber and chemical components

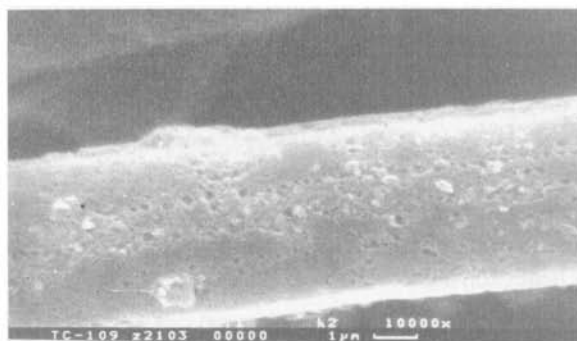
Compression of 'Busofit' with a binder (salt) could help to minimize a void space (Eq. 1) and increase the sorption capacity of the active carbon fiber. If the carbon material is compounded with metal hydride/chloride microcrystals disposed in the same volume, it could facilitate to handle the problem of the efficient gas storage and transportation.

The developed sorbent complex compound microstructure has been analyzed using Scanning Electro Microscope. The porous structure with a uniform distribution of salt crystals without formation of agglomerates or large particle size distribution were observed [12].

The results of the experimental analysis of the sorption capacity of the active carbon fiber 'Busofit' and complex compound – 'Busofit' + calcium chloride are presented in Figure 7, and Table 3 (the data are obtained for the room temperature, except methane (253 K)). 'Busofit' has a typical micropores distribution mostly on the filament surface. A set of microcrystals of metal hydrides/chlorides is attached on the filament surface also (as shown in Figure 8). Combination 'Busofit' + metal hydrides have some particularities to compare with the combination 'Busofit' + metal chlorides. Due to the high density of metal hydrides, the systems tend to be very compact. However, the relatively low metal hydrides hydrogen capacity leads to considerable weight of the systems. Thus, metal hydride applications are best suited for systems where power and volume are more critical than weight. A hydrogen compressor, or storage reservoir based on the reversible solid sorption phenomenon is advantageous if the process can provide high gas density, the reactor contains a large quantity of the reactive media, and the kinetic of the gas-solid reaction is sufficiently fast. Heat and mass transfer processes are rapid and effective if the reactor material has good porosity and high thermal conductivity. In the case of gas-salt reaction, the use of the salt-binder compound (carbon, powdered and expanded graphite, graphite intercalation compounds and intercalated or impregnated carbon fibers) could enhance the energy and power performances of the system. Another solution is impregnated carbon fabrics saturated with metal hydrides for hydrogen storage. Successful application in practical systems

Table 4. *Metal hydride materials for the hydrogen storage and transportation*

Metal hydride	Suitable as sorbent	Technical storage capacity, kg/kg	Temperature, K
LaNi <sub>4.1</sub> Al <sub>0.52</sub> Mn <sub>0.37</sub>	Yes	0.007–0.009	430–490
LaNi <sub>4.5</sub> Al <sub>0.29</sub> Mn <sub>0.21</sub>	Yes	0.008–0.01	373–433
LmNi <sub>4.91</sub> Sn <sub>0.15</sub>	Yes	0.01	279–303
Ti <sub>0.9</sub> Zr <sub>0.10</sub> V <sub>0.43</sub> Fe <sub>0.09</sub> Cr <sub>0.09</sub> Mn <sub>1.5</sub>	Yes	0.01	283–323
Ti <sub>0.99</sub> Zr <sub>0.01</sub> V <sub>0.43</sub> Fe <sub>0.09</sub> Cr <sub>0.05</sub> Mn <sub>1.5</sub>	Yes	0.01	268–303

Figure 8. 'Busofit' filaments covered by CaCl<sub>2</sub> microcrystals. Image multiplied by 50,000 times.

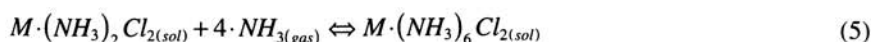
requires particular properties of the hydride alloys. Good alloy candidates (Table 4) must have proper temperature and pressure interval, high total uptake of hydrogen and energy density of the material. The pressure plateau must also be in the range of the system operational conditions.

Metal hydride reaction beds inside the storage vessel can be temperature controlled (for instance, by heat pipe heat transfer devices), or pressure controlled (isobaric).

During the gas adsorption stage the reactor solid material (metal chloride/hydride) reacts with the gas by following exothermic reaction:



This chemical reaction is reversible, and for example, in the case of transition metal chloride MCl<sub>2</sub> (S) and ammonia (G), the following reaction could be observed:



The enthalpy of reaction  $\Delta H_{react}$  in (5) is about 50 kJ/mol ammonia. The poor thermal conductivity of the solid salt (about 0.1 W/(m·K)) and the very high expansion factor of the salt S during the gas adsorption, are two crucial parameters being able to reduce the sorption capacity. Heat has to be evacuated during the chemical adsorp-

tion reaction, and gas diffusion to the reacting media has not to be slackened. Conversely, in the regeneration (desorption) phase, the reactor operates as regenerator and the reaction is endothermic.

The use of additives (active carbon fiber) to metal chloride/hydride has two functions:

- the increase of the total sorption capacity (adsorption + chemisorption)
- the increase of the reactant effective thermal conductance and the heat transfer coefficient at the interface between reactant and wall
- the maintenance of the high permeability of the medium during the solid-gas reaction.

The addition of carbon powders, graphite compounds, expanded graphite, activated carbons, carbon fibers, carbon fabrics to metal chloride/hydride enhance the performances of the gas storage vessel. It is particularly convenient to use carbon fabrics because they possess the following properties:

- 2D high thermal conduction (if the precursor fibers have good thermal conductivity),
- high gas permeability into the inter-fibers space,
- absence of the thermal conductivity discontinuities (gaps) between the reactor core and the heat exchanger wall.

The metal hydride + 'Busofit' gas storage vessel can also be considered as a heat sink for the transport vehicle, or the source of energy for the air conditioning system. The heat sink absorbs and rejects metabolic, sun and equipment heat loads generated during the car transportation.

#### 4. Heat and mass transfer in the sorbent bed

Complex compound reactor can be used in conjunction with heat pipe thermal control system. The element of sorbent bed with heat pipe as the thermal control unit for gas storage vessel (GSV) is shown in Figure 9. The element is bounded by the outer surface of the vessel ( $r = R$ ), the inner wall of the vessel ( $r = R_0$ , heat pipe wall), and the planes of symmetry passing through the center of the fin ( $z = 0$ ) and the center of the sorbent bed ( $z = S$ ) between two nearby fins.

The mathematical model of heat transfer and gas sorption processes in the cylindrical reactor is based on the following assumptions: 1) the pressure in the cylinder is uniform; 2) the resistance to the mass diffusion is small; 3) the temperature of the solid phase is equal to the temperature of the gas phase at each point, because of the high coefficient of the volumetric heat transfer between them; 4) the gas in the cylinder is ideal; 5) the heat energy used on compressing or expanding gas is not taken into account; 6) gas is flowing in the radial direction through the sorbent bed.

The dynamic modeling of the sorbent bed includes the following components [11]:

1. Dubinin-Radushkevich gas equation (2);
2. the equation of energy:

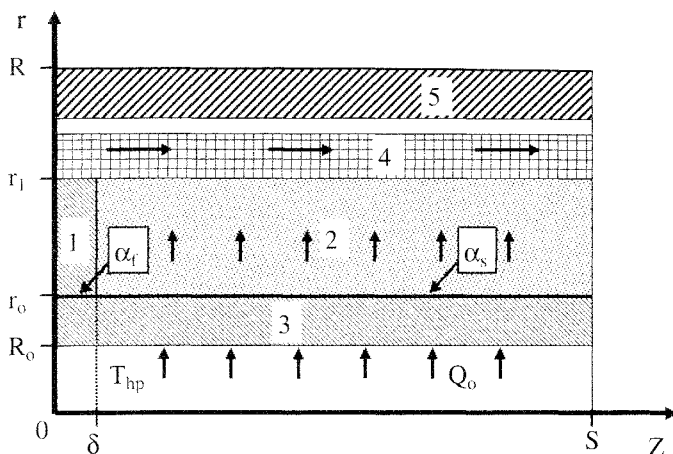


Figure 9. Diagram of the calculated element of the GSV: 1 – fin; 2 – sorbent; 3 – shell of the heat pipe; 4 – channel for gas discharge formed by the perforated tube and the cylinder body; 5 – cylinder body.

$$r(\varepsilon C_g + \rho C + \rho a C_a) \frac{\partial T}{\partial \tau} + r c v C_g \frac{\partial T}{\partial r} = \frac{\partial}{\partial r} \left( r \lambda \frac{\partial T}{\partial r} \right) + \frac{\partial}{\partial z} \left( r \lambda \frac{\partial T}{\partial z} \right) + r q_{st} \rho \frac{\partial a}{\partial \tau}, \quad (6)$$

$$\text{where the isosteric heat of sorption is: } q_{st} = R_\mu T \left[ \frac{\partial \ln P}{\partial \ln T} \right]_{|a=\text{const}}; \quad (7)$$

3. the equation of continuity:

$$r \frac{\partial T}{\partial \tau} (\varepsilon c + \rho a) + \frac{\partial}{\partial z} (r c v) = 0; \quad (8)$$

4. the equation of sorption kinetic:

$$\frac{da}{d\tau} = K_{s0} \exp \left( -\frac{E}{R_\mu T} \right) (a_{eq} - a), \quad (9)$$

where  $K_{s0} = 15 D_{s0} / R_p^2$ ,  $R_p$  – radii of the particle.  $D_{s0}$  – constant necessary to determine the coefficient of a surface diffusion,  $D_s = D_{s0} \exp[E/(R_\mu T)]$

The solution was found for the fixed gas flow from the GSV

$$2\pi \frac{d}{d\tau} \int_{\delta}^S \int_{r_0}^{r_1} (\varepsilon a + \rho a) r dr dz = -G/N \quad (10)$$

with boundary conditions (Figure 9):

$$P|_{\tau=0} = P_0; \quad T(r, z)|_{\tau=0} = T_0(r, z) = T_{env}; \quad (11)$$

$$\left. \frac{\partial T}{\partial z} \right|_{z=0} = 0, \quad \left. \frac{\partial T}{\partial z} \right|_{z=S} = 0; \quad -\lambda \left. \frac{\partial T}{\partial r} \right|_{r=R} = \alpha_{env}(T - T_{env}), \quad (12)$$

$$-\lambda \left. \frac{\partial T}{\partial r} \right|_{r=R_0} = \frac{Q_{hp}}{2\pi R_0 SN}, \quad \text{or} \quad T|_{r=R_0} = T_{hp}, \quad (13)$$

where  $Q_{hp}$  – heat flow used to heat one cylinder of the GSV,  $T_{hp}$  – gas vessel wall temperature.

The first condition in equation (13) relates to the case when the power  $Q_{hp}$  is known, and the second condition corresponds to the situation when the heating power is not limited but the temperature  $T_{hp}$  is determined. This constant temperature could be maintained at the inner surface of the heat pipe due to the thermal contact of its evaporator with a large heated body, such as an engine.

To solve the set of equations (2, 6–9) with boundary conditions (11–13) the method of finite elements for fixed mesh [12, 13] was used. The number of triangular elements in the calculated region was from 200 to 300. Convergence precision was equal to  $10^{-6}$ . In-house program package was developed in Visual Fortran.

The suggested simple model gives us a possibility to obtain the field of temperature and gas concentrations during charge-discharge procedure of the gas vessel.

## 5. Heat pipe heat exchangers

Sorbent bed can be used as a compact sandwich with flat or cylindrical heat pipes being in good thermal contact with an available source of energy (for example, gas flame, electric heater, solar concentrator, etc.). Various types of heat pipes: conventional heat pipes, heat pipe panels, loop heat pipes, vapour-dynamic thermosyphons and other two phase evaporation/condensation heat transfer devices were developed and used for sorbent bed thermo control at Luikov Heat and Mass Transfer Institute [14–17].

Heat pipes can easily be implemented inside sorption storage vessels due to its flexibility, high heat transfer efficiency, cost-effectiveness, reliability, long operating life, and simple manufacturing technology.

Conventional heat pipes (Figure 10) are suitable as heat transfer devices for sorption bed layer thermal control [14–16]. A very important feature of heat pipe is its ability to transport large amounts of energy over the length of heat pipe with a small temperature drop by means of liquid evaporation at the evaporator (heat source) and vapor condensation at the condenser (heat sink) and liquid movement in the opposite direction inside a wick by capillary or body forces. Essential point is a possibility to reverse the direction of a heat flow along the heat pipe in time and to use same heat pipe for cooling and heating alternatively.

For some applications pulsating flat heat pipe panels [17] have advantages over conventional cylindrical heat pipes. The space-efficient arrangement, ability of the quick dissipation of the localized heat, and the maintenance of high-isothermal flat surface are very important (Figures 10, 11). The liquid-vapour interface formed in

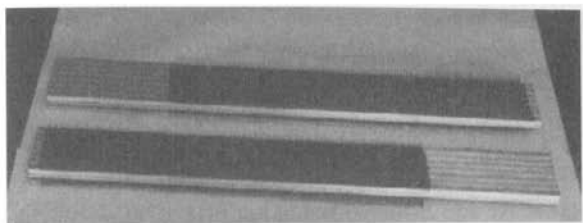


Figure 10. *Pulsating heat pipe panels for sorbent bed thermal control.*

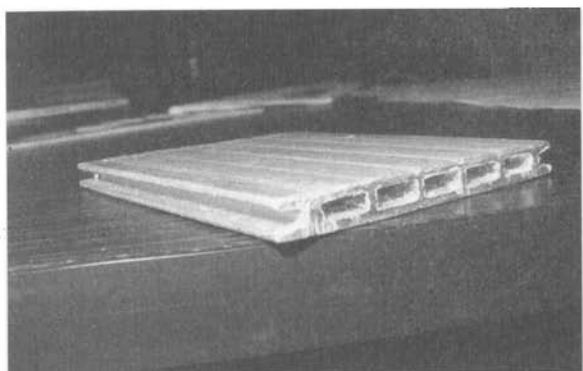


Figure 11. *Element of pulsating heat pipe panel.*

capillary channels inside the heat pipe panel is capable to generate self-sustained thermally driven oscillations. Thin layer (several mm) of the sorbent between mini-fins on the outer side of the heat pipe panel ensures an advanced heat and mass transfer during the cycle adsorption/desorption.

Heat pipe panel (HPP) is filled partially with working fluid. The flow instabilities inside are generated during multi-channels ( $H = 2$  mm,  $L = 5$  mm) heating at one end and simultaneously cooling the other end. The instabilities are resulting in fluid pulsating. This heat input and output arrangement forms a heat transfer mechanism, as a combination of sensible and latent heat portions. The fluid pulsations are a superposition of various underlying effects.

In our research project an aluminium multi-channel panel was chosen as an experimental set-up (Figures 10, 11). The main parameters of the pulsating flat heat pipe panel, developed in the Luikov Institute are: HPP width – 70 mm, HPP height – 7 mm, HPP length – 700 mm, evaporator length – 98 mm, condenser length – 500 mm, mass – 0.43 kg. Propane was selected as working fluid because of its excel-



lent compatibility with majority heat pipe envelopes and wick materials (aluminium, steel, stainless steel, copper,  $Al_2O_3$ , etc).

## 6. Conclusions

To improve the parameters of the gas storage system a new sorbent material, a complex compound based on the combination of activated carbon fiber and metal hydride/chloride with the binder, was suggested. The composition active carbon fiber and metal chloride/hydride micro crystals have two functions: to increase the total sorption capacity (adsorption + chemisorption) and the maintenance of a high permeability of the medium during the solid-gas reactions.

The application of heat pipes in gas storage vessel allows efficiently controlling sorbent bed temperature, rate and direction of the reaction, and to provide optimal operational conditions.

The complex compounds have a good potential as a major element of a novel gas storage systems for hydrogen vehicles.

## References

- [1] S. Hynek, W. Fuller and J. Bentley, 'Hydrogen storage by carbon sorption', *Int. J. Hydrogen Energy*, 22 (1997), 601–610.
- [2] C. Carpetis and W. Peschka, 'A study on hydrogen storage by use of cryoadsorbents', *Int. J. Hydrogen Energy*, 5 (1980), 539–554.
- [3] H. M. Cheng, Q. H. Yang and C. Liu, 'Hydrogen storage in carbon nanotubes', *Int. J. Hydrogen Energy*, 27 (2002), 193–202.
- [4] A. V. Kuznetsov and K. Vafai, 'Analytical comparison and criteria for heat and mass transfer models in metal hydrides packed beds', *Int. J. Hydrogen Energy*, 38 (1995), 2873–2884.
- [5] L. L. Vasiliev, D. A. Mishkinis, A. A. Antukh and L. L. Vasiliev Jr., 'Solar – Gas solid sorption refrigerator', *Adsorption*, 7 (2001), 149–161.
- [6] K. J. Chang and O. Talu, 'Behavior and performance of adsorptive natural gas storage cylinders during discharge', *Appl. Therm. Eng.*, 16 (1996), 359–374.
- [7] L. L. Vasiliev, A. G. Kulakov, D. A. Mishkinis, A. M. Safonova and N. K. Luneva, 'Activated Carbon For Gas Adsorption' in *3d Int. Symposium on Fullerene and Semifullerene Structures in the Condensed Media*, Minsk, Belarus, 22–25 June, 2004, 110–115.
- [8] L. L. Vasiliev, L. E. Kanonchik, D. A. Mishkinis and M. I. Rabetsky, 'Adsorbed natural gas storage and transportation vessels', *Int. J. Therm. Sci.*, 39 (2000), 1047–1055.
- [9] M. M. Dubinin, 'The potential theory of adsorption of gases and vapors for sorbents with energetically nonuniform surfaces', *Chem. Rev.*, 60 (1960), 235–241.
- [10] R. K. Agarwal, *High Pressure Adsorption of Pure Gases on Activated Carbon: Analysis of Adsorption Isotherms by Application of Potential Theory and Determination of Heats and Entropies of Adsorption*. Ph. D. Dissertation, Syracuse, 1988.
- [11] L. L. Vasiliev, L. E. Kanonchik, D. A. Mishkinis and M. I. Rabetsky, 'A new method of Methane Storage and Transportation', *Int. J. Environmentally Conscious Design & Manufacturing*, 9 (2000), 35–62.
- [12] O. Zenkevich, *Method of Finite Elements in Engineering* [in Russian], Moscow, 1976.
- [13] V. P. Maltsev and V. P. Maiboroda, *Calculation of Machine-Building Constructions by the Method of Finite Elements* [in Russian], Moscow, 1989.
- [14] L. L. Vasiliev, A. G. Kulakov and D. A. Mishkinis, 'Activated carbon for gas adsorption' in *Int. Conference Solid State Hydrogen Storage – Materials and Applications*, Hyderabad, India., 2005, 10–18.

- [15] L. L. Vasiliev and A. G. Kulakov, 'Heat Pipe applications in sorption refrigerators, low temperature and cryogenic refrigeration', *NATO Science Series II*, 99 (2003), Kluwer Academic Publishers, 401–414.
- [16] L. L. Vasiliev, 'Heat pipes in modern heat exchangers', *Appl. Therm. Eng.*, 25 (2005), 1–19.
- [17] A. A. Antukh, M. I. Rabetsky, V. F. Romanenkov and L. L. Vasiliev, 'Pulsating heat pipe panels' in Hou Zengqi, Shao Xingguo, Yao Wei (ed.), *Heat Pipe Theory and Applications*, (Shanghai, China, 2004), 491–497.

# International Journal of Low Carbon Technologies

**Contents** Volume 1 Number 2 April 2006

**Activated carbon fiber composites for ammonia, methane and hydrogen adsorption**

L. L. Vasiliev, L. E. Kanonchik, A. G. Kulakov, D. A. Mishkinis, A. M. Safonova and N. K. Luneva

**Designing a hybrid wind and solar energy supply system for a rural residential building**

M.-A. Hessami

**Development of a simple intermittent absorption solar refrigeration system**

J. K. Tangka and N. E. Kamnang

**Experimental investigation of energy storage for an evacuated solar collector**

S. B. Riffat, L. Jiang, J. Zhu and G. Gan

**Investigation of a novel small-scale solar desalination plant**

A. K. Lalzad, I. W. Eames, G. G. Maidment and T. G. Karayiannis

**Investigations on effect of the orientation on thermal comfort in terraced housing in Malaysia**

M. Ali. Al-Obaidi and P. Woods

**Reflectance distributions and atrium daylight levels: a comparison between physical scale model and Radiance simulated study**

S. Samant and B. Medjdoub

**The Seawater Greenhouse: background, theory and current status**

P. A. Davies and C. Paton

**MANCHESTER**  
1824

Manchester University Press

ISSN 1748-1317



[www.manchesteruniversitypress.co.uk](http://www.manchesteruniversitypress.co.uk)